

## Article

# Lyapunov-Based Impact Time Control Guidance Law with Performance Prediction

Hyeong-Geun Kim <sup>1</sup> and Jongho Shin <sup>2,\*</sup><sup>1</sup> Department of Mechanical Engineering, Incheon National University, Incheon 22012, Republic of Korea<sup>2</sup> School of Mechanical Engineering, Chungbuk National University, Cheongju 28644, Republic of Korea

\* Correspondence: jshin@cbnu.ac.kr; Tel.: +82-43-261-2447

**Abstract:** This paper proposes an impact time control guidance law based on exact nonlinear kinematics equations. To address the impact time control problem of providing enhanced intercept accuracy, we formulated an error variable whose regulation ensures the fulfillment of the required tasks without time-to-go estimation. Based on the Lyapunov stability theory, a desired line-of-sight rate profile that satisfies the convergence of the error variable was constructed, from which the guidance command was designed using the optimal tracking formulation. The simple structure of the proposed guidance law enables the prediction of interceptor behavior during homing, thereby allowing the interceptor to maneuver along feasible trajectories. In addition, although the structure of the proposed guidance law is simple and similar to that of proportional navigation, it is theoretically guaranteed to execute the required mission precisely at the end of homing. Numerical simulations demonstrated that the proposed guidance law achieved effective target interception under various terminal constraint settings.

**Keywords:** homing guidance; impact time control guidance; Lyapunov stability theory; closed-loop analysis



**Citation:** Kim, H.-G.; Shin, J. Lyapunov-Based Impact Time Control Guidance Law with Performance Prediction. *Aerospace* **2023**, *10*, 308. <https://doi.org/10.3390/aerospace10030308>

Academic Editor: Gokhan Inalhan

Received: 14 February 2023

Revised: 13 March 2023

Accepted: 17 March 2023

Published: 20 March 2023



**Copyright:** © 2023 by the authors. Licensee MDPI, Basel, Switzerland. This article is an open access article distributed under the terms and conditions of the Creative Commons Attribution (CC BY) license (<https://creativecommons.org/licenses/by/4.0/>).

## 1. Introduction

Proportional navigation (PN) guidance, which is designed to nullify the line-of-sight (LOS) rate with simple proportional control, has been used extensively due to its satisfactory performance and uncomplicated structure [1]. In particular, pure PN with a navigation constant of 3 is considered an optimal solution that effectively minimizes the quadratic summation of the normal acceleration for engagement against a stationary target [2]. However, with the widespread use of anti-air defense systems in modern warfare, it is becoming increasingly difficult to achieve accurate interception with PN aimed at minimizing only the miss distance to the target. For example, it is difficult for a PN-guided missile to cause significant damage to a warship armed with close-in weapon systems.

A simultaneous attack by synchronizing the arrival time of multiple missiles on a single target is an effective strategy that can neutralize anti-air defense systems. To satisfy such requirements, feedback control on the arrival time of each missile should be performed, which is referred to as impact time control guidance (ITCG). Since ITCG was first introduced [3], a number of studies have investigated various guidance formulations [3–20].

Linearization for engagement kinematics based on small-angle approximation has been widely utilized, which makes it easier to design guidance laws by replacing the original nonlinear equation. The guidance laws presented in pioneering ITCG studies [3,4] were also derived by linearized kinematics based on the small-angle approximation to the flight path angle to realize the easy application of the optimal control theory. As an extended version, a subsequent guidance law [5] was structured as a polynomial function, where coefficients were determined according to the boundary conditions of the impact angle and time constraints. Here, linearized equations were exploited in the process of determining the values of the coefficients.

To exploit the advantage of simplifying equations and reducing the intercept inaccuracies caused by the approximation, several previous studies have partially implemented linearization in the design of guidance laws. The primary representative example of such partial linearization is the time-to-go estimation [6–11]. In these studies, the time-to-go, whose exact value cannot be measured in real-world engagement scenarios, was calculated under the assumption that the missile was guided by PN based on the linearized kinematics. However, unlike the linear guidance laws provided in the literature [3–5], these laws were designed based on accurate engagement equations and nonlinear control theories (except for deriving the time-to-go calculation), i.e., nonlinear optimal theory [6], the Lyapunov stability theory [7–9], and sliding mode control [10,11]. Thus, more accurate ITCG performance was expected compared to the linearized-kinematics-based guidance laws.

Recently, ITCG laws derived from exact nonlinear equations without approximation have been studied to eliminate errors caused by linearization. The main focus of such studies was determining how to handle the time-to-go factor, which must be estimated precisely, and recent studies have adopted two main approaches, i.e., accurate time-to-go estimation [12–14] and the exclusion of time-to-go [15–20]. The studies presented in [12–14] proposed PN-based guidance structures, where nonlinear closed-loop solutions were derived to calculate the exact expression of the time-to-go. With these guidance structures, the exact fulfillment of ITCG was guaranteed due to the exclusion of linearization; however, the resulting expression of the guidance law included an incomplete beta function, which is a rather complicated function.

To ensure accurate performance with a simple structure, previous studies [15–20] excluded the use of the time-to-go in the configuration of the guidance law. For example, a previous study [15] utilized a tracking method to follow the desired heading error profile rather than defining the impact time error. Note that successful tracking guarantees the satisfaction of the impact time constraint; thus, the guidance law achieves ITCG without estimating the time-to-go. A similar approach that constructs a look angle profile in polynomial form has also been adopted [16]. In addition, in a previous study [17], a virtual heading error was defined based on the characteristics of the arc trajectory without considering the time-to-go. Here, as convergence to the virtual heading error guaranteed the impact time control, the guidance law could avoid using the time-to-go in the implementation. In another study [18], conditions based on the engagement geometry were proposed to ensure that the designated impact time could be achieved, and this concept was extended in a subsequent study [19] that presented the necessary and sufficient conditions to ensure interception at the required impact time even for moving targets. The two-stage guidance law provided in [20] achieved the required impact time by adjusting the switching point between each stage, and the appropriate switching point was determined using the Newton iteration method.

The nonlinear guidance laws presented in [12–20] ensure the accurate fulfillment of ITCG due to their precise consideration of the exact governing equations. In particular, the ITCG laws presented in the literature [15–20] ensure that the required tasks can be achieved even with simple structures by avoiding the estimation of the time-to-go. However, unlike linear methods [3–5] with simpler structures, such nonlinear guidance laws exhibit a distinct disadvantage, i.e., the closed loop is difficult to investigate analytically due to the complicated nonlinearity. In addition, with guidance laws involving a numerical iterative routine [20], it is particularly difficult to analyze the closed-loop characteristics. Thus, it is difficult to prevent such nonlinear guidance laws from generating a command that makes the interceptor perform maneuvers along impractical trajectories.

Thus, in this paper, we propose a guidance law that attempts to satisfy ITCG based on exact nonlinear governing equations. As the first step to consider the ITCG problem, we constructed a desired profile of the look angle. Here, the required tasks were guaranteed to be achieved based on the Lyapunov stability theory. We then utilized an optimal tracking method to derive an effective guidance law that tracked the desired profile. In all these processes, the time-to-go estimation was not included. In addition, by using an

approximation technique that did not degrade the terminal performance of the guidance law, we could obtain an explicit solution for the closed-loop equations, providing helpful analysis for practical implementation, e.g., the expected trajectory and maximum value of the required command input.

Compared to the existing ITCG laws, the proposed guidance law yields the following contributions. First, from a theoretical perspective, the proposed guidance law fully guarantees the achievement of ITCG, because the convergence of the defined variable ensures interception at the designated time without the need to calculate the time-to-go. Here, the use of nonlinear engagement equations constructed without approximation supports such theoretical guarantees.

Another contribution of the proposed guidance law is that it provides an explicit closed-loop solution for the engagement kinematics; thus, it is possible to predict the future behavior of the interceptor. Although the small-angle approximation of the look angle is required to derive the closed-loop solution, this does not negatively affect the terminal accuracy of homing, because the convergence of the look angle to zero is guaranteed. In addition, this closed-loop solution does not involve highly complex transcendental functions, e.g., a Gaussian geometric function or incomplete beta function.

In addition, the proposed guidance law does not require an iterative routine, e.g., numerical optimization or the Newton–Raphson method. In other words, the proposed guidance law is expected to be more suitable for practical implementation than numerical computation-based guidance laws.

The remainder of this paper is organized as follows. Section 2 describes the nonlinear formulation of the engagement kinematics as the groundwork to design the ITCG law. In Section 3, the proposed nonlinear formulation-based guidance law is presented to solve the ITCG problem. Then, in Sections 4 and 5, the performance of the proposed guidance law is investigated according to the analytic closed-loop solution and numerical simulations, respectively. Finally, concluding remarks are presented in Section 6.

## 2. Problem Statement

Here, we assume the engagement scenario illustrated in Figure 1, where missile  $M$  moving at velocity  $V_M$  and normal acceleration  $a_M$  attempts to intercept the stationary target  $T$ . In Figure 1,  $r$  and  $\lambda$  represent the relative range and the LOS angle, and  $\gamma_M$  and  $\sigma_M$  denote the flight path angle and look angle of the missile to the target, respectively. Thus, the relative motion of the missile with respect to the target is governed by the following equations:

$$\dot{r} = -V_M \cos \sigma_M \quad (1)$$

$$r\dot{\lambda} = -V_M \sin \sigma_M \quad (2)$$

$$\dot{\sigma}_M = \frac{a_M}{V_M} + \frac{V_M \sin \sigma_M}{r} \quad (3)$$

The primary objective of an ITCG law is to achieve interception at the designated impact time  $t_d$ , which is expressed as follows:

$$r(t_d) = 0 \quad (4)$$

The key condition for the ITCG is presented in the form of a boundary condition, as shown in (4); thus, it is difficult to apply a general control algorithm that regulates a specified variable in a straightforward manner. Therefore, we introduced error variable  $e_t$ , whose convergence guarantees target interception at the designated time, as follows:

$$e_t = V_M t_{go}^d - r \quad (5)$$

Here,  $t_{go}^d$  is the desired time-to-go, defined as  $t_{go}^d = t_d - t$ . Then, we obtained the following proposition:

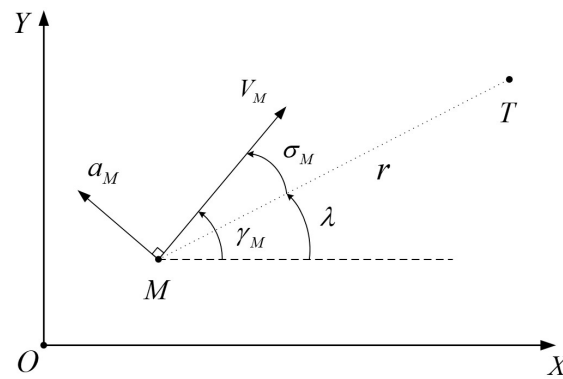


Figure 1. Two-dimensional engagement geometry for a stationary target.

**Proposition 1.** Suppose that a missile, whose engagement kinematics are governed by (1)~(3), is guided by an arbitrary guidance law that maintains  $e_t = 0$ , where  $e_t$  is defined by (5). Then, the missile is guaranteed to achieve the condition in (4), i.e., the impact time control guidance is fulfilled.

**Proof.** Taking the time derivative to  $e_t$  generates the following:

$$\frac{de_t}{dt} = -V_M + V_M \cos \sigma_M \tag{6}$$

which indicates that the maintenance of  $e_t = 0$  is equivalent to  $\sigma_M = 0$ . Then, the missile is guaranteed to move in a straight line toward the target; the time-to-go is entirely determined as  $t_{go} = r/V_M$  without the need to estimate. Therefore,  $e_t = 0$  implies that the missile reaches the target at an impact time of  $t = t_d$ , which verifies (4). □

Thus, the design of a controller that achieves  $e_t = 0$  is equivalent to the development of an ITCG law. Herein, the Lyapunov stability theory and optimal tracking method were utilized to achieve this design objective, which is described in detail in Section 3.

**Remark 1.** Generally, the desired impact time  $t_d$  is set to be greater than  $r(0)/V_M$ , which is the minimum value of the expected impact time. Thus, it is obvious that the initial value of the error variable  $e_t$  is always positive.

### 3. Design of Impact Time Control Guidance Law

As presented in the following, we designed the ITCG law in two steps. First, as the groundwork to design the guidance law, a desired profile of the look angle was structured based on the error dynamics of  $e_t$  provided in (6). Subsequently, we employed the optimal tracking method, which was proposed in a preliminary study [21], to design the ITCG law.

From the error dynamics of the impact time in (6), we defined the desired profile of the look angle to achieve  $e_t = 0$  as follows:

$$\sigma_M^d = k\sqrt{\frac{e_t}{r}} \tag{7}$$

Here,  $k$  is a gain selected as a positive constant. Assume that the error dynamics in (6) are evolved by the desired look angle in (7). Then, the substitution of  $\sigma_M = \sigma_M^d$  into (6) yields the following equation:

$$\frac{de_t}{dt} = -V_M + V_M \cos\left(k\sqrt{\frac{e_t}{r}}\right) \tag{8}$$

In relation to (8), we present the following lemmas.

**Lemma 1.**  $e_t$  is always non-negative during homing for an initial condition of  $e_t(0) > 0$ .

**Proof.** Suppose that  $e_t$  can become negative. Then,  $e_t$  should pass zero because it starts with a positive value. However, from (8), it is verified that  $e_t = 0$  is an attractor, because  $de_t/dt|_{e_t=0} = 0$  is achieved. This implies that  $e_t$  can never escape from  $e_t = 0$  once  $e_t$  reaches zero, which contradicts the assumption that  $e_t$  can become negative.  $\square$

**Lemma 2.**  $e_t = 0$  is the only attractor for (8).

**Proof.** We begin with the assumption that (8) has more than one attractor. Note that the attractor candidates must satisfy  $\cos(k\sqrt{e_t}/r) = 1$ , which is equivalent to:

$$k^2 e_t = 4n^2 \pi^2 r \tag{9}$$

where  $n$  can be a non-zero positive integer due to the assumption. By differentiating both sides with respect to time, we obtain the following:

$$\begin{aligned} k^2 \left\{ -V_M + V_M \cos\left(k\sqrt{\frac{e_t}{r}}\right) \right\} &= -4n^2 \pi^2 V_M \cos\left(k\sqrt{\frac{e_t}{r}}\right) \\ \Leftrightarrow 0 &= -4n^2 \pi^2 V_M \end{aligned} \tag{10}$$

which contradicts the idea that  $n$  can be a non-zero positive integer.  $\square$

Using Lemmas 1 and 2, we could verify that  $e_t = 0$  is achieved by the desired look angle in (7) with the following proposition.

**Proposition 2.**  $e_t$  is guaranteed to converge to zero in (8). In addition,  $e_t = 0$  is ensured to be achieved as  $r$  approaches zero.

**Proof.** Here, we define the Lyapunov candidate function of  $V_t \triangleq e_t^2/2$ . Taking the time derivative to the candidate function provides the following:

$$\dot{V}_t = \left\{ -V_M + V_M \cos\left(k\sqrt{\frac{e_t}{r}}\right) \right\} e_t \tag{11}$$

In (11),  $e_t$  is always non-negative, as proved by Lemma 1. In addition, from Lemma 2, it can be inferred that we only need to analyze the convergence for the domain of  $[-\pi, \pi]$  for the cosine function. Thus,  $\dot{V}_t$  satisfies the following:

$$\begin{aligned} \dot{V}_t &\leq \left\{ -V_M \frac{2}{\pi^2} \left(k\sqrt{\frac{e_t}{r}}\right)^2 \right\} e_t \\ &= -\frac{2V_M k^2 e_t^2}{\pi^2 r} \leq 0 \end{aligned} \tag{12}$$

where the mathematical relationship of  $\cos x \leq 1 - (2/\pi^2)x^2 \forall x \in [-\pi, \pi]$  is utilized. The result in (12) proves that  $e_t$  converges to zero. In addition, the actual time-to-go, which is defined as  $t_{go} = t_f - t$ , is always greater than or equal to  $r/V_M$ , i.e., the time taken for a straight flight. Thus,  $\dot{V}_t$  in (12) satisfies the following:

$$\dot{V}_t \leq -\frac{2k^2 e_t^2}{\pi^2 t_{go}} = \frac{4k^2}{\pi^2} \frac{V_t}{t_f - t} \tag{13}$$

which provides

$$V_t \leq V_t(0) \left(\frac{t_f - t}{t_f}\right)^{-4k^2/\pi^2} \tag{14}$$

The result of (14) proves that  $e_t$  converges to zero as homing is terminated.  $\square$

Proposition 2 implies that the ITCG task is satisfied if the actual look angle converges to the desired profile  $\sigma_M^d$  before homing ends. Here, we used the finite-time tracking method that designs the nonlinear optimal solution for achieving  $\sigma_M = \sigma_M^d$ , which was previously proposed in a preliminary study in [21]. To apply the tracking method, we established the LOS rate error, defined as  $e_\lambda \triangleq \dot{\lambda} - \dot{\lambda}_d$ , where  $\dot{\lambda}_d$  is the desired LOS rate for the ITCG, defined as  $\dot{\lambda}_d \triangleq -V_M \sin \sigma_M^d / r$ . Then, to consider the terminal boundary condition of  $r = 0$  easily in the error equation, we set the error dynamics for  $e_\lambda$  with respect to the relative range  $r$  as follows:

$$\frac{de_\lambda}{dr} = \frac{a_M}{V_M r} - 2\frac{\dot{\lambda}}{r} - \frac{d\dot{\lambda}_d}{dr} \quad (15)$$

where (1) is used. Then, by applying the tracking method [21], we constructed the guidance command as follows:

$$a_M = a_M^{eq} + a_M^{cont} \quad (16)$$

where  $a_M^{eq}$  is an equivalent term to compensate for the parts that are relevant to the desired LOS rate given by:

$$a_M^{eq} = 2V_M \dot{\lambda}_d + V_M r \frac{d\dot{\lambda}_d}{dr}. \quad (17)$$

Note that the controller term  $a_M^{cont}$  in (16) was designed by the optimal theory such that its quadratic summation was minimized, as shown by the following proposition.

**Proposition 3** ([21]). *Consider the following quadratic performance index:*

$$J(r_0) = \int_0^{r_0} \frac{1}{2\bar{r}^m} u^2(r) dr \quad (18)$$

where  $r_0$ ,  $m$ , and  $u(r)$  are the initial values of the relative range, the guidance gain selected as a positive constant, and the feedback control input defined as  $u(r) = a_M^{cont}(r) / V_M$ , respectively. Then, the optimal solution to minimize (18) subject to the dynamic constraint of (15) and the desired boundary condition of  $e_\lambda(0) = 0$  is written as follows:

$$a_M^{cont}(r) = (m+3)V_M e_\lambda(r_0) \left(\frac{r}{r_0}\right)^{m+1} \quad (19)$$

where  $e_\lambda(r_0)$  is the initial value of the LOS rate error. In addition, the real-time feedback command, in which the current state variables (rather than their initial values) are used as the boundary conditions, is obtained as follows:

$$a_M = (m+3)V_M \dot{\lambda} - (m+1)V_M \dot{\lambda}_d + V_M r \frac{d\dot{\lambda}_d}{dr}. \quad (20)$$

The proof for Proposition 3 can be found in Proposition 1 and Remark 1 in [21]. As the convergence of  $\sigma_M = \sigma_M^d$  before the end of homing is proven by Proposition 3, we deduced that  $e_t = 0$  is also achieved during homing. As a result, it was theoretically verified that the guidance law proposed in (7) and (20) achieves target interception at the designated impact time  $t_d$ .

#### 4. Analysis of Proposed Guidance Law

In this section, we investigate the performance of the proposed guidance law via closed-loop analysis to determine whether the proposed law produces feasible results in a realistic context. In Section 4.1, we obtain a closed-loop solution using the small-angle approximation under the proposed command input. Based on the calculated closed-loop solution, the future behavior of the engagement variables and guidance commands

for the given boundary conditions and parameter settings are predicted to evaluate the applicability of the proposed law, in Sections 4.2 and 4.3, respectively.

#### 4.1. Approximated Closed-Loop Solution

By applying the guidance law proposed in (20) to the engagement equations, we analyzed the closed-loop behavior according to the following proposition.

**Proposition 4.** Using the small-angle approximation, the look angle  $\sigma_M$ , which varies by the command proposed in (20), can be expressed as a polynomial function for the relative range as follows:

$$\sigma_M = c_m r^{m+2} + c_n r^n \quad (21)$$

where  $n$  is defined as  $n = (k^2 - 2)/4$ , and the constant coefficients  $c_m$  and  $c_n$  are determined by the given boundary condition.

**Proof.** First, we derived the closed-loop solution for the desired profile of the look angle. From (8), we obtained the closed-loop dynamics of the error variable  $e_t$  with respect to the relative range  $r$  as follows:

$$\frac{de_t}{dr} = \sec\left(k\sqrt{\frac{e_t}{r}}\right) - 1 \quad (22)$$

both  $e_t$  and  $de_t/dr$  converge to zero before the end of homing, as proven by Lemma 2 and Proposition 2; thus, the small-angle approximation of  $\sec(k\sqrt{e_t/r}) \approx 1 + (k\sqrt{e_t/r})^2/2$ , which is based on the Taylor approximation, does not deteriorate the terminal accuracy of the closed-loop analysis. Thus, we obtained the following approximated error dynamics for  $e_t$ :

$$\frac{de_t}{dr} = \frac{k^2}{2} \frac{e_t}{r} \quad (23)$$

which provided the solution of

$$e_t(r) = e_t(r_0) \left(\frac{r}{r_0}\right)^{k^2/2}. \quad (24)$$

By combining (7) and (24), we obtained the closed-loop solution for  $\sigma_M^d$  as follows:

$$\sigma_M^d = c_n r^n \quad (25)$$

where parameter  $n$  is defined as  $n = (k^2 - 2)/4$ , and coefficient  $c_n$  is determined by the boundary condition. From the result of (25), we could confirm that the desired look angle is expressed as a power function of the relative range; however, this did not mean that the actual look angle has the form of a power function. To investigate the behavior of the actual look angle, we identified the entire closed-loop according to the following procedure.

By substituting (20) into the error dynamics of (15), we obtained the following:

$$\frac{de_\lambda}{dr} = (m+1) \frac{e_\lambda}{r} \quad (26)$$

which yielded the following solution for  $\lambda(r)$ .

$$\lambda(r) = \lambda_d(r) + e_\lambda(r_0) \left(\frac{r}{r_0}\right)^{m+1} \quad (27)$$

With the small-angle approximation for  $\sigma_M$ , which is ensured to converge to zero, we obtained the solution for the actual look angle as follows:

$$\sigma_M(r) = c_m r^{m+2} + c_n r^n \quad (28)$$

To calculate the values of  $c_m$  and  $c_n$ , we set the approximated equation for  $e_t$  as follows:

$$\frac{de_t}{dr} = \sec \sigma_M - 1 \approx \frac{1}{2} \sigma_M^2 \quad (29)$$

where (1) and (6) are involved. Here, by integrating both sides of (29) using (28), we obtained the following:

$$e_t(r) = \frac{c_m^2}{2(2m+5)} r^{2m+5} + \frac{c_n^2}{2(2n+1)} r^{2n+1} + \frac{c_m c_n}{m+n+3} r^{m+n+3} \quad (30)$$

Then, by applying the boundary conditions of  $\sigma_M(r_0)$  and  $e_t(r_0)$  to (28) and (30), respectively, the coefficients were computed as follows:

$$c_m = \frac{(2m+5)\sigma_M(r_0) + \sqrt{-(2m+5)(2n+1)\sigma_M^2(r_0) + 4(2m+5)(2n+1)(m+n+3)\frac{e_t(r_0)}{r_0}}}{2(m-n+2)r_0^{m+2}}$$

$$c_n = \frac{-(2n+1)\sigma_M(r_0) - \sqrt{-(2m+5)(2n+1)\sigma_M^2(r_0) + 4(2m+5)(2n+1)(m+n+3)\frac{e_t(r_0)}{r_0}}}{2(m-n+2)r_0^{m+2}} \quad (31)$$

Note that the coefficients in (31) were selected from two roots of the quadratic equation to satisfy the condition  $\sigma_M(r) \geq 0$ .  $\square$

Due to the simple polynomial structure of the look angle expressed in (28), the future behavior of the state variable and command input could be predicted from the given boundary conditions. In the following sections, we utilized such predictions to estimate the arrival angle and the maximum magnitude of the command input.

#### 4.2. Trajectory Analysis

The arrival angle at the missile's target can be an effective measure to determine whether a proposed law produces a practically feasible trajectory. For example, if the missile approaches the target with an arrival angle near  $-90^\circ$ , a vertical strike is attainable to maximize the attack's lethality; otherwise, if a trajectory is generated with a positive arrival angle, it would be difficult to reach the target in a real-world implementation.

The arrival angle, which is also referred to as the impact angle, can be calculated as the final value of the LOS angle for a stationary target. For this calculation, we applied the polynomial form of the look angle in (28) to the LOS dynamics, formulated as follows:

$$\frac{d\lambda}{dr} \approx \frac{\sigma_M}{r} \quad (32)$$

where (1) and (2) are used with the small-angle approximation for  $\sigma_M$ . By solving (32) with the substitution of (28), we obtained the following expression for the arrival angle  $\lambda_f$ :

$$\lambda_f = \lambda(r_0) - \frac{c_m}{m+2} r_0^{m+2} - \frac{c_n}{n} r_0^n \quad (33)$$

where  $\lambda(r_0)$  denotes the initial value of the LOS angle. The result of (33) allows the user to identify whether the proposed law generates an implementable trajectory by predicting the arrival angle before homing. Such results would be useful when applying the proposed guidance law to an engagement scenario against both terrestrial and naval targets.

#### 4.3. Acceleration Command Analysis

The closed-loop analysis conducted in Section 4.1 could be utilized to predict the maximum magnitude of the command input of the proposed guidance law. Here, by replacing  $\dot{\lambda}$  and  $\dot{\lambda}_d$  in (20) with the obtained closed-loop solution of (25) and (27), respectively, we obtained the following additional form of the guidance command:

$$a_M(r) = -V_M^2 \left\{ (m + 3)c_m r^{m+1} + (n + 1)c_n r^{n-1} \right\} \tag{34}$$

where the approximations of  $\sin \sigma_M \approx \sigma_M$  and  $\sin \sigma_M^d \approx \sigma_M^d$  are used. Note that both  $\sigma_M$  and  $\sigma_M^d$  are guaranteed to converge to zero at the end of homing; thus, such approximations do not deteriorate the terminal accuracy. The result of (34) provides two useful points. First, if  $m$  and  $n$  are selected to satisfy  $m > -1$  and  $n > 1$ , the generated command from  $a_M$  converges to zero at the end of homing. Thus, it is recommended to select guidance gains under such conditions to realize the stable terminal performance of the autopilot system. Next, we could predict the maximum magnitude of  $a_M(r)$  during homing by obtaining the critical point  $r_2$  that satisfies  $da_M/dr|_{r=r_2} = 0$  as follows:

$$r_2 = \left( -\frac{(n + 1)(n - 1)c_n}{(m + 3)(m + 1)c_m} \right)^{1/(m-n+2)} \tag{35}$$

If no real root exists for  $r_2$  in (35), it can be inferred that the initial value is the maximum of  $|a_M|$  during the entire homing process; otherwise, the maximum magnitude for  $a_M(r) \forall r \in [0, r_0]$  was determined as follows:

$$\max_{r \in [0, r_0]} |a_M(r)| = \max(|a_M(r_0)|, |a_M(r_2)|). \tag{36}$$

Using the result of (36), it becomes possible to preselect appropriate guidance gains to achieve the required tasks while considering the maximum maneuverable limit of the given autopilot system. This is expected to be beneficial for the practical implementation of the proposed law, as with the analysis of the arrival angle.

### 5. Simulation Results

Here, we evaluate the performance of the proposed guidance law. In Section 5.1, the primary characteristics of the proposed law are investigated by conducting engagement simulations under various settings. Then, in Section 5.2, the performance of the proposed law is compared to that of existing ITCG laws to validate the contributions of this study. To consider the time delay effect caused by missile dynamics and autopilot, a first-order system with a time constant of 0.1 s is applied in all simulations, and the maximum magnitude of the normal acceleration is assumed to be saturated as  $|a_M| \leq 10$  g. The corresponding simulation parameters, boundary conditions, and desired constraints are listed in Table 1.

**Table 1.** Simulation parameters.

Parameter	Value
Initial position of missile, $(x_M(0), y_M(0))$	(0, 0) km
Position of stationary target, $(x_T, y_T)$	(10, 0) km
Missile speed, $V_M$	250 m/s
Desired impact time, $t_d$	50 s, 60 s, 70 s
Guidance gains, $(m, n)$	(0, 1), (1, 2), (2, 3)

#### 5.1. Performance Analysis

Figure 2a–c show the results obtained using the proposed guidance law with gains of  $(m, n) = (0, 1), (1, 2),$  and  $(2, 3)$ , respectively. Here, the gain  $k$  to construct  $\sigma_M^d$  in (7) was determined to satisfy  $n = (k^2 - 2)/4$ , as described in Proposition 4. As shown in Figure 2a,b, the proposed guidance law under various gain settings achieved target interception at the designated impact time by regulating both error variables,  $e_t$  and  $e_\lambda$ . Specifically, an impact time of  $t_f = 49.99$  s was achieved in all cases. In addition, the trajectory exhibited a larger curvature in the initial stage as  $m$  and  $n$  increased, which was due to the fact that the proposed guidance law expresses the look angle as a polynomial function with  $m$  and  $n$  as exponents despite being based on the nonlinear Lyapunov stability

theory, as verified by Proposition 4. Note that the look angle histories shown in Figure 2c also support this analysis. The lower part of Figure 2c, where the produced command is plotted, shows that the proposed guidance law generated an acceleration command that converged to zero when the gains were set to  $m > 0$  and  $n > 1$ , because the command could be approximated as a polynomial with exponents of  $m + 1$  and  $n - 1$ , as verified in Section 4.3. Thus, it is advantageous to select gains that satisfy such conditions so that the command converges to zero.

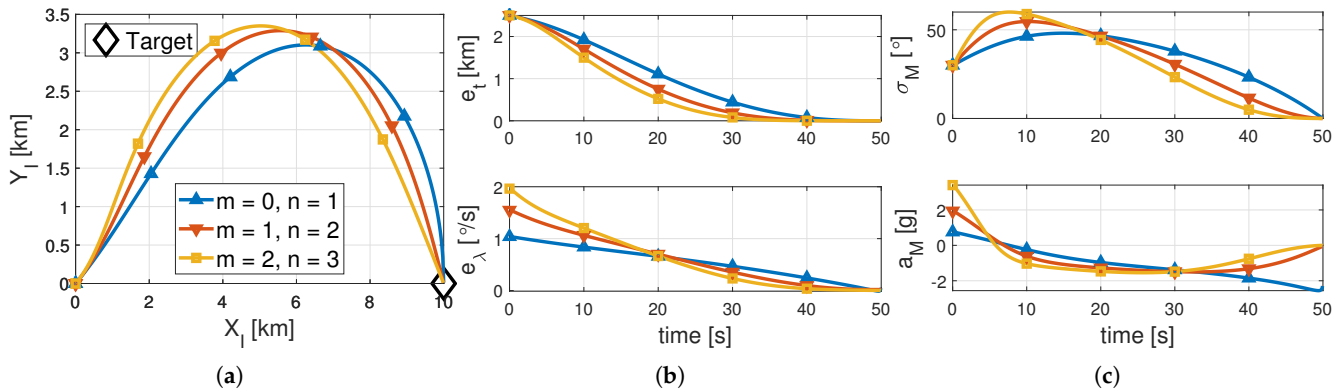


**Figure 2.** Simulation results under the proposed law with gains of  $(m, n) = (0, 1), (1, 2),$  and  $(2, 3)$ . (a) Flight trajectories; (b) error variables; (c) state and input variables.

Figure 3a–c show the engagement results obtained using the proposed law for the designated impact times of  $t_d = 50$  s,  $60$  s, and  $70$  s, respectively, with fixed gains of  $m = 2$  and  $n = 3$ . Here, Figure 3a,b show that the proposed guidance law made the error variables converge to zero before homing ended, as proven by Propositions 2 and 3. In addition, the specific impact time for each case was  $t_f = 49.99$  s,  $59.99$  s, and  $69.99$  s, which indicates that the proposed guidance law satisfied ITCG with an accuracy within  $|t_f - t_d| \leq 1 \times 10^{-2}$  s. In addition, the predicted arrival angles for the  $t_d = 50$  s,  $60$  s, and  $70$  s cases were calculated as  $-51.41^\circ$ ,  $-73.89^\circ$ , and  $-91.04^\circ$ , which did not deviate considerably from the actual arrival angles of  $-50.51^\circ$ ,  $-74.34^\circ$ , and  $-95.08^\circ$ , respectively. By applying the estimation of (36) to this scenario, it was predicted that the maximum magnitude of the guidance command would occur at the initial point in all cases, which was consistent with the actual results shown in Figure 3c. In addition, due to the gain setting of  $m = 2$  and  $n = 3$ , we observed that the proposed guidance law generated a command that converged to zero in all cases.

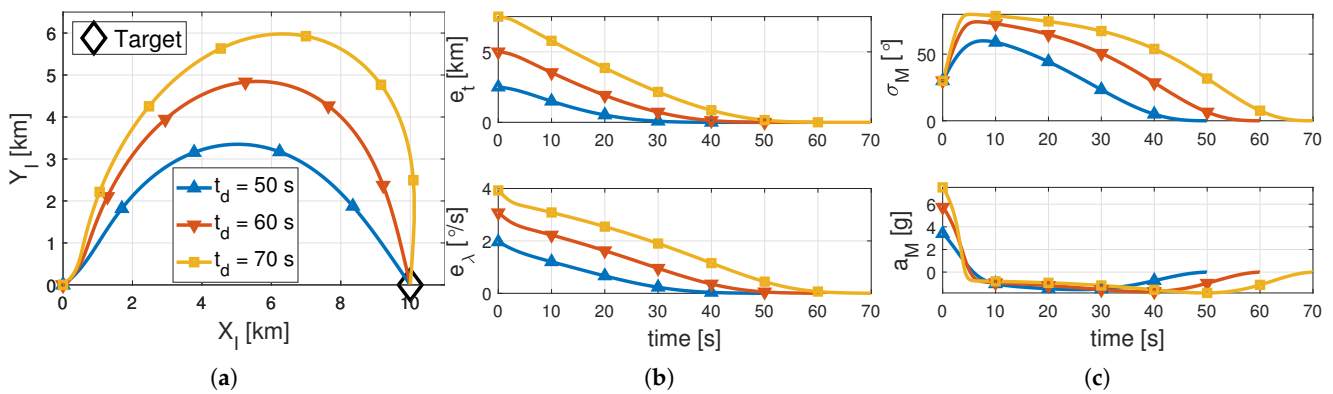


**Figure 3.** Simulation results under the proposed law for the desired constraint of  $t_d = 50$  s,  $60$  s, and  $70$  s. (a) Flight trajectories; (b) error variables; (c) state and input variables.

## 5.2. Comparative Studies

To facilitate an effective comparative analysis, the performance of the proposed law was compared to that of existing nonlinear ITCG laws, i.e., the nonlinear optimal guidance (NOG) law [6] and the range-polynomial guidance (RPG) law [16]. Here, the NOG and RPG laws were applied to generate the following commands:

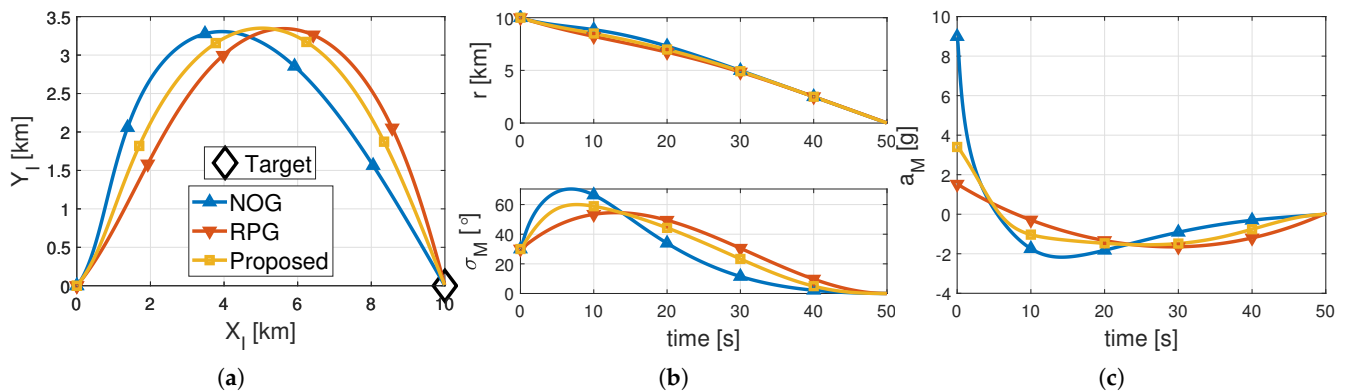
$$\text{NOG} : a_M = NV_M \dot{\lambda} + N(N+1)(2N-1) \frac{V_M^5}{NV_M \dot{\lambda} r^3} (t_{go}^d - t_{go}^{PNG}) \quad (37)$$

$$\text{RPG} : a_M = \kappa_c V_M (t_d - t)^2 - \frac{2V_M \sigma_M}{t_d - t} + V_M \dot{\lambda} \quad (38)$$

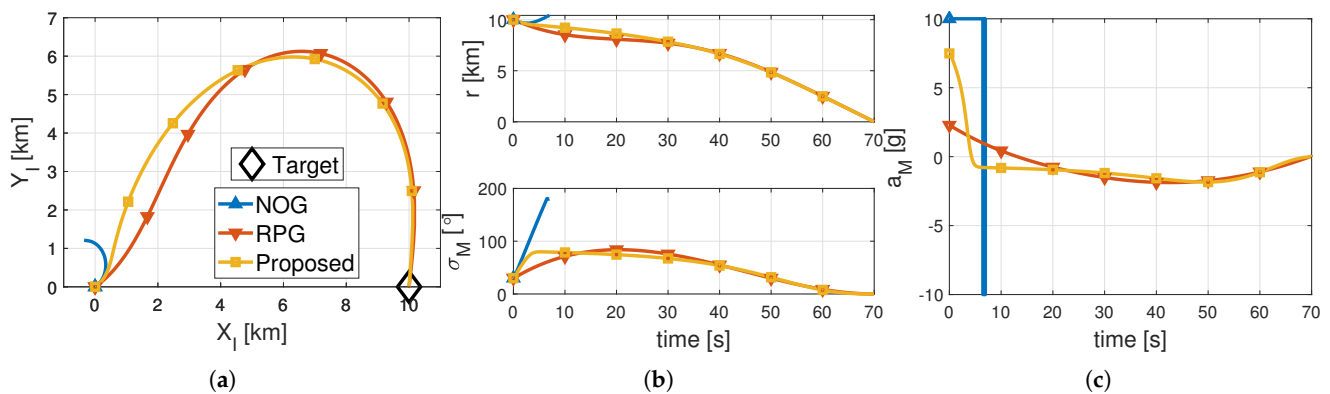
Note that detailed discussions regarding the parameter selections can be found in the respective literature.

Figure 4a–c show the results obtained by the three guidance laws for the desired impact time of  $t_d = 50$  s. As shown in Figure 4a,b, all three compared laws satisfied the interception at the required impact time. The specific interception results obtained by NOG, RPG, and the proposed guidance law were  $t_f = 49.99$  s,  $49.99$  s, and  $49.99$  s, respectively. The accurate accomplishment of the required tasks by all three guidance laws was attributed to the precise consideration of engagement kinematics based on nonlinear equations. In particular, RPG and the proposed guidance law were designed to satisfy sufficient conditions for ITCG without estimating the time-to-go; thus, achieving the required missions was ensured theoretically.

By virtue of such features, both RPG and the proposed guidance law satisfied the required impact time of  $t_d = 70$  s with a time of  $t_f = 69.99$  s, as shown in Figure 5a–c; however, we found that NOG failed to intercept the target, as the command oscillated between each limit. This divergence was caused by the convergence of  $\dot{\lambda}$  to zero before  $t_{go}^d$  converged to  $t_{go}^{PNG}$ , as shown in (37). In contrast, the closed-loop analysis presented in each study validated that both NOG and the proposed guidance law produced commands in the form of polynomial functions that did not diverge. Thus, it is expected that RPG and the proposed guidance law could be applied more reliably in practical implementation than the NOG law.



**Figure 4.** Simulation results under NOG, RPG, and the proposed law for the desired constraint of  $t_d = 50$  s. (a) Flight trajectories; (b) state variables; (c) guidance commands.



**Figure 5.** Simulation results under NOG, RPG, and the proposed law for the desired constraint of  $t_d = 70$  s. (a) Flight trajectories; (b) state variables; (c) guidance commands.

In addition, unlike RPG, which requires a numerical root-finding routine to compute the guidance gain  $\kappa_c$ , the proposed guidance law can be implemented with only an analytical calculation. In other words, no numerical iterative computation is required, even for the prediction of the future behavior of the proposed guidance law, as described in Section 4. Thus, we concluded that the proposed guidance law is superior to RPG and NOG in terms of both performance reliability and the ease of practical implementation.

## 6. Conclusions

Herein, we have proposed a Lyapunov-based ITCG law that provides performance prediction by analyzing the closed-loop. In the proposed guidance law, we first formulate the error variable, which ensures that target interception can realize the designated impact time despite the lack of time-to-go estimation. Here, error regulation is achieved by constructing the desired command of the LOS rate, where performance is validated according to the Lyapunov stability theory. In addition, the acceleration command is configured as a nonlinear controller that tracks the presented LOS rate command by applying an optimal tracking formulation developed in a previous study. The proposed guidance law is proven to yield a trajectory that takes the form of a polynomial function of the relative range, which allows us to predict the expected performance, e.g., the arrival angle and maximum magnitude of the command input. Although the small-angle approximation for the look angle is utilized to predict the expected behavior of the proposed guidance law, this does not reduce terminal accuracy because the look angle is guaranteed to converge to zero. In addition, no approximation is involved in the design of the proposed guidance law, and the achievement of the required terminal constraints is verified; thus, fulfillment of ITCG is ensured theoretically. Finally, comparative investigations conducted via numerical simulations have effectively demonstrated and validated the important contributions of the proposed guidance law.

**Author Contributions:** Methodology, H.-G.K.; Investigation, J.S.; Writing—original draft, H.-G.K.; Writing—review & editing, J.S. All authors have read and agreed to the published version of the manuscript.

**Funding:** This work was supported by Incheon National University Research Grant in 2020.

**Data Availability Statement:** Not applicable.

**Conflicts of Interest:** The authors declare no conflict of interest.

## References

1. Zarchan, P. *Tactical and Strategic Missile Guidance*, 5th ed.; AIAA, Inc.: Reston, VA, USA, 2007; pp. 11–29.
2. Jeon, I.S.; Lee, J.I. Optimality of proportional navigation based on nonlinear formulation. *IEEE Trans. Aerosp. Electron. Syst.* **2010**, *46*, 2051–2055. [[CrossRef](#)]
3. Jeon, I.S.; Lee, J.I.; Tahk, M.J. Impact-time-control guidance law for anti-ship missiles. *IEEE Trans. Control Syst. Technol.* **2006**, *14*, 260–266. [[CrossRef](#)]
4. Lee, J.I.; Jeon, I.S.; Tahk, M.J. Guidance law to control impact time and angle. *IEEE Trans. Aerosp. Electron. Syst.* **2007**, *43*, 301–310.
5. Kim, T.H.; Lee, C.H.; Jeon, I.S.; Tahk, M.J. Augmented polynomial guidance with impact time and angle constraints. *IEEE Trans. Aerosp. Electron. Syst.* **2013**, *49*, 2806–2817. [[CrossRef](#)]
6. Jeon, I.S.; Lee, J.I.; Tahk, M.J. Impact-time-control guidance with generalized proportional navigation based on nonlinear formulation. *J. Guid. Control Dyn.* **2016**, *39*, 1885–1890. [[CrossRef](#)]
7. Zhang, Y.; Wang, X.; Wu, H. Impact time control guidance law with field of view constraint. *Aerosp. Sci. Technol.* **2014**, *39*, 361–369. [[CrossRef](#)]
8. Kim, M.; Jung, B.; Han, B.; Lee, S.; Kim, Y. Lyapunov-based impact time control guidance laws against stationary targets. *IEEE Trans. Aerosp. Electron. Syst.* **2015**, *51*, 1111–1122. [[CrossRef](#)]
9. Zhang, Y.; Wang, X.; Wu, H. Impact time control guidance with field-of-view constraint accounting for uncertain system lag. *Proc. Inst. Mech. Eng. Part G J. Aerosp. Eng.* **2016**, *230*, 515–529. [[CrossRef](#)]
10. Kumar, S.R.; Ghose, D. Impact time guidance for large heading errors using sliding mode control. *IEEE Trans. Aerosp. Electron. Syst.* **2015**, *51*, 3123–3138. [[CrossRef](#)]
11. Cho, D.; Kim, H.J.; Tahk, M.J. Nonsingular sliding mode guidance for impact time control. *J. Guid. Control Dyn.* **2016**, *39*, 61–68. [[CrossRef](#)]
12. Cho, N.; Kim, Y. Modified pure proportional navigation guidance law for impact time control. *J. Guid. Control Dyn.* **2016**, *39*, 852–872. [[CrossRef](#)]
13. Lee, S.; Cho, N.; Kim, Y. Impact-Time-Control Guidance Strategy with a Composite Structure Considering the Seeker’s Field-of-View Constraint. *J. Guid. Control Dyn.* **2020**, *43*, 1566–1574. [[CrossRef](#)]
14. Kim, H.G.; Lee, H. Composite Guidance for Impact Time Control Under Physical Constraints. *IEEE Trans. Aerosp. Electron. Syst.* **2022**, *58*, 1096–1108. [[CrossRef](#)]
15. Tekin, R.; Erer, K.S.; Holzapfel, F. Control of impact time with increased robustness via feedback linearization. *J. Guid. Control Dyn.* **2016**, *39*, 1682–1689. [[CrossRef](#)]
16. Tekin, R.; Erer, K.S.; Holzapfel, F. Polynomial shaping of the look angle for impact-time control. *J. Guid. Control Dyn.* **2017**, *40*, 2668–2673. [[CrossRef](#)]
17. Chen, X.; Wang, J. Nonsingular sliding-mode control for field-of-view constrained impact time guidance. *J. Guid. Control Dyn.* **2018**, *41*, 1214–1222. [[CrossRef](#)]
18. Kim, H.G.; Kim, H.J. Backstepping-based Impact Time Control Guidance Law for Missiles with Reduced Seeker Field-of-View. *IEEE Trans. Aerosp. Electron. Syst.* **2019**, *55*, 82–94. [[CrossRef](#)]
19. Kim, H.G.; Cho, D.; Kim, H.J. Sliding mode guidance law for impact time control without explicit time-to-go estimation. *IEEE Trans. Aerosp. Electron. Syst.* **2019**, *55*, 236–250. [[CrossRef](#)]
20. Wang, C.; Yu, H.; Dong, W.; Wang, J. Three-Dimensional Impact Angle and Time Control Guidance Law Based on Two-Stage Strategy. *IEEE Trans. Aerosp. Electron. Syst.* **2022**, *58*, 5361–5372. [[CrossRef](#)]
21. Kim, H.G.; Lee, J.Y. Generalized Guidance Formulation for Impact Angle Interception with Physical Constraints. *Aerospace* **2021**, *8*, 307. [[CrossRef](#)]

**Disclaimer/Publisher’s Note:** The statements, opinions and data contained in all publications are solely those of the individual author(s) and contributor(s) and not of MDPI and/or the editor(s). MDPI and/or the editor(s) disclaim responsibility for any injury to people or property resulting from any ideas, methods, instructions or products referred to in the content.